Mathematics

Research article

Multiple solitons with bifurcations, lump waves, M-shaped and interaction solitons of three component generalized (3+1)-dimensional Breaking soliton system

Saleh Mousa Alzahrani[*] **and Talal Alzahrani**

Department of Mathematics, University College in Al-Qunfudhah, Umm Al-Qura University, Al-Qunfudhah, Saudi Arabia

* **Correspondence:** Email: salzahrani@uqu.edu.sa.

Abstract: The generalized (3+1)-dimensional Breaking soliton system (gBSS) has numerous applications across various scientific fields. This manuscript presents a study on important exact solutions of the gBSS, with a focus on novel solutions. Using the Hirota bilinear technique, we derive the general solution of the proposed system and obtain the novel solutions by considering different types of auxiliary functions. Our analysis includes the study of multi-solitons, multiple bifurcation solitons, lump wave solutions, M-shaped solitons, and their interactions. We also observe several hybrid solitons, including tuning fork-shaped, X-Y shaped, and double Y shaped. Our results are presented through graphical representations.

1. Introduction

The accurate analysis and interpretation of mechanisms and events in various nonlinear systems arising in fluid mechanics, nonlinear optical fibers and applied sciences heavily relies on the discovery of exact solutions of nonlinear equations. Various methods have been utilized by scholars to identify exact solutions of several types to nonlinear partial differential equations (PDEs). In the quest to analyze PDE solitons, researchers have utilized a range of analytical methods that includes inverse scattering approach [1], reduction methods [2], ansatz technique [3], and other techniques [4]. The bilinear method is powerful technique used to find analytic solutions to PDEs of nonlinear type. Bilinear method is often referred to as the Hirota bilinear method, a term coined after Hirota's original proposal in 1971. Bilinear type operators are unique type of Backlund transformations which gives a

unified approach to finding the Backl··und transformation solutions of the PDEs. This is primary concept of the manuscript. The bilinear method has since evolved to create more comprehensive solutions, including lumps [5], breathers [6], rogue waves [7], and other interaction solutions [8, 9]. Further, Cheng et al have studied N-solitons of the (2+1)-D generalized KdV model in [10]. Similarly for some more useful and excellent works on asymptotics for solitons in large order limit, the reader is referred to [11, 12]. We consider the following three component nonlinear (3 + 1)-dimensional generalized breaking soliton system (gBSS) [13]

$$\mathcal{W}_t + \alpha \mathcal{U}_{xxx} + \beta \mathcal{U}_{xxy} + \gamma \mathcal{U}\mathcal{U}_x + \lambda \mathcal{U}\mathcal{U}_y + \delta \mathcal{U}_x \mathcal{V} = 0,$$
$$\mathcal{W}_x = \mathcal{U}_x + \mathcal{U}_y + \mathcal{U}_z, \mathcal{U}_y = \mathcal{V}_x,$$

(1.1)

where α is a constant. The (3+1)-dimensional gBSS is a mathematical model that describes the behavior of nonlinear waves in three-dimensional space and time. It consists of three components: dispersion, nonlinearity, and dissipation. Dispersion refers to the spreading of waves, nonlinearity refers to the interaction between waves, and dissipation refers to the loss of energy by waves. These three components interact to produce a variety of phenomena, such as soliton formation and wave breaking.

Whenever two or more than two solitons overlap, and interact in evolution system, they can either collide elastically or pass through each other. During a soliton-soliton collision, the solitons maintain their amplitude, speed, and path, except for a phase shift. This behavior is due to the balance between nonlinearity and dispersion, which allows the solitons to interact without changing their properties.

Nonlinear physical systems can support multiple solitons that can coexist and interact with each other. The interaction between solitons is a natural response of the system and can lead to complex dynamics. The shapes and arrangements of natural phenomena such as plants, streams, mountains, and many others can fall into a vast category of naturally occurring phenomena known as bifurcation. Bifurcation refers to the emergence of complex behavior from the interaction between multiple solitons, leading to the creation of intricate patterns and structures. Solitons capable of splitting or combining during soliton interactions are called bifurcation solitons, and they can effectively replicate the bifurcation phenomenon of nonlinear processes. Recently, a Y-type soliton, the simplest bifurcation soliton, was discovered by two-soliton fusion [14, 15]. In physics, lump wave refer to a type of wave solution that behaves like a localized lump or a pulse of energy that travels through a medium. These waves can arise in nonlinear systems where the wave speed depends on the amplitude of the wave, leading to wave packets that retain their shape and energy as they propagate. In mathematics, the term may refer to a particular type of solution of partial differential equations, such as the Korteweg–de Vries equation, which describes the propagation of nonlinear waves in dispersive media [16, 17]. The lump wave solution of this equation is a localized solution that behaves like a soliton, maintaining its shape and speed over time. Overall, the concept of lump wave solutions has important applications in various fields, including physics, mathematics, and engineering. In [18], researchers presented the dynamics bright as well as dark lump solutions for a novel BKP-Boussinesq model in (3+1)-dimensions. Additionally, lump and rogue waves for Broer Kaup Kupershmidt model is studied by the authors in [19]. The coexistence of rogue waves, M-shaped solitons, and other types of solitons were reported in [20].

2. Bilinear form

Here we present the bilinear form (BF) of the suggested system. To calculate BF of the proposed Eq (1.1), in [13] authors have selected $\lambda = \delta = 3\beta$ and $\gamma = 6\alpha$, then substituting these into Eq (1.1), and obtained the following

$$\partial_x^{-1}(\mathcal{U}_{xt} + \mathcal{U}_{zt} + \mathcal{U}_{yt}) + \beta\mathcal{U}_{xxy} + \alpha\mathcal{U}_{xxx} + 6\alpha\mathcal{U}\mathcal{U}_x + 3\beta\mathcal{U}_x\partial_x^{-1}\mathcal{U}_y + 3\beta\mathcal{U}\mathcal{U}_y = 0. \qquad (2.1)$$

Now upon the substitution of $\mathcal{U} = \phi_x = 2(\ln \Upsilon)_{xx}$ and $\mathcal{V} = \phi_y = 2(\ln \Upsilon)_{xy}$, where $\phi = \varpi_x = 2(\ln \Upsilon)_x$, Υ, ϕ and ϖ are real functions of (x, y, z, t), the following bilinear form is obtained

$$\alpha\Upsilon\Upsilon_{xxxx} - 4\alpha\Upsilon_x\Upsilon_{xxx} + 3\alpha\Upsilon_{xx}^2 + \beta\Upsilon\Upsilon_{xxxy} - \beta\Upsilon_{xxx}\Upsilon_y - 3\beta\Upsilon_x\Upsilon_{xxy} + 3\beta\Upsilon_{xx}\Upsilon_{xy}$$
$$+ \Upsilon\Upsilon_{xt} - \Upsilon_x\Upsilon_t + \Upsilon\Upsilon_{yt} - \Upsilon_y\Upsilon_t + \Upsilon\Upsilon_{zt} - \Upsilon_z\Upsilon_t = 0. \qquad (2.2)$$

In Hirota $\mathcal{D}$−operator form above equation can be written as

$$(\mathcal{D}_x\mathcal{D}_t + \mathcal{D}_y\mathcal{D}_t + \mathcal{D}_z\mathcal{D}_t + \alpha\mathcal{D}_x^4 + \beta\mathcal{D}_x^3\mathcal{D}_y)\Upsilon.\Upsilon = 0.$$

Where the $\mathcal{D}$−operator is defined as

$$\prod_{\sigma=1}^{Q} \mathcal{D}_{x_\sigma}^{\zeta_\sigma} \mathbb{A}.\mathbb{B} = \prod_{\sigma=1}^{Q} \left(\frac{\partial}{\partial x_\sigma} - \frac{\partial}{\partial x'_\sigma}\right)^{\zeta_\sigma} \mathbb{A}(x)\mathbb{B}(x')\,|_{x'=x}, \qquad (2.3)$$

where $x = (x_1, x_2, \ldots, x_{\mathcal{K}})$, $x' = (x'_1, x'_2, \ldots, x'_Q)$, denotes vectors and $\zeta_1, \zeta_2, \ldots, \zeta_Q \in Z^+$. There will be two various types of exact solutions for the suggested equation which are presented below

$$\mathcal{U} = 2\frac{\Upsilon_{xx}\Upsilon - (\Upsilon_x)^2}{\Upsilon^2}, \qquad (2.4)$$

$$\mathcal{V} = 2\frac{\Upsilon_{xy}\Upsilon - \Upsilon_x\Upsilon_y}{\Upsilon^2}. \qquad (2.5)$$

3. First order soliton

Here we begin the study on soliton solutions from the first order soliton of proposed model Eq (1.1), first we calculate constraint condition. In order to calculate the constraint condition we consider the following function

$$Q = e^{\mathcal{K}_\varsigma}, \qquad (3.1)$$

where

$$\mathcal{K}_\varsigma = \varrho_\varsigma x + \zeta_\varsigma y + \gamma_\varsigma z - \lambda_\varsigma t, \; \varsigma \in Z^+. \qquad (3.2)$$

Now inserting Eq (3.1) in Eq (1.1) except nonlinear terms, and after doing so solving the resulting equation for λ_ς, we get

$$\lambda_\varsigma = \frac{\varrho_\varsigma^4\alpha + \varrho_\varsigma^3\zeta\beta}{\varrho_\varsigma + \zeta_\varsigma + \gamma_\varsigma}, \qquad (3.3)$$

for obtaining soliton of the first order, one can consider auxiliary function Υ as follows

$$\Upsilon = 1 + e^{\mathcal{K}_1}, \tag{3.4}$$

where $\mathcal{K}_1 = \varrho_1 x + \zeta_1 y + \gamma_1 z - \lambda_1 t$, putting Eq (3.4) into Eqs (2.4) and (2.5) repectively we obtained the first order soliton solutions as follows

$$\mathcal{U} = \frac{\varrho_1^2}{1 + \cosh(\mathcal{K}_1)}. \tag{3.5}$$

$$\mathcal{V} = \frac{\varrho_1 \zeta_1}{1 + \cosh(\mathcal{K}_1)}. \tag{3.6}$$

Equation (3.5) is visualized in Figure 1a, while the exact solution Eq (3.6) is presented in Figure 1b, where one soliton is observed.
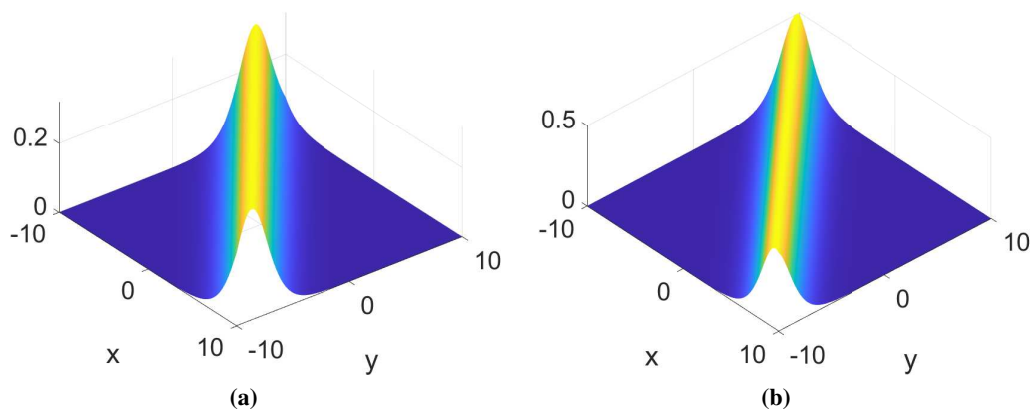
Figure 1. The 3D dynamics of the first-order soliton solutions Eqs (3.5) and (3.6) with parameters used as $z = 1$, $t = 1$, $\rho_1 = 0.8$, $\zeta_1 = 1$, $\gamma_1 = 1$, $\alpha = 1$, $\beta = 1$.

4. Second order soliton with bifurcation

Here, we find the soliton solution of second order. Therefore we take the Υ as sum of the two exponential functions and its product in the form of

$$\Upsilon = 1 + e^{\mathcal{K}_1} + e^{\mathcal{K}_2} + \Re_{12} e^{\mathcal{K}_1 + \mathcal{K}_2}, \tag{4.1}$$

here the $\mathcal{K}_\varsigma$, with $\varsigma = 1, 2$ can be obtained from the Eq (3.2). Next we put Eq (4.1) into Eq (2.2) and solve the obtained result for the dispersion coefficient (DC) $\Re_{12}$, hence we get

$$\Re_{12} = \frac{\mathcal{P}_{12}\lambda_1 + \mathcal{Q}_{12}\lambda_2 + (\varrho_1^4 + \varrho_2^4)\alpha + (-4\varrho_1^2 + 6\varrho_1\varrho_2 - 4\varrho_2)\varrho_1\varrho_2\alpha + (\varrho_1 - \varrho_2)^3(\zeta_1 - \zeta_2)\beta}{\mathcal{R}_{12}(\lambda_1 + \lambda_2) - (\varrho_1^4 + \varrho_2^4)\alpha + (-4\varrho_1^2 - 6\varrho_1\varrho_2 - 4\varrho_2^2)\varrho_1\varrho_2\alpha - (\varrho_1 - \varrho_2)^3(\zeta_1 + \zeta_2)\beta}, \tag{4.2}$$

where $\mathcal{P}_{12} = -\varrho_1 + \varrho_2 - \zeta_1 + \zeta_2 - \gamma_1 + \gamma_2$, $\mathcal{Q}_{12} = \varrho_1 - \varrho_2 + \zeta_1 - \zeta_2 + \gamma_1 - \gamma_2$ and $\mathcal{R}_{12} = \varrho_1 + \varrho_2 + \zeta_1 + \zeta_2 + \gamma_1 + \gamma_2$. In more general format the Eq (4.2) can be written as

$$\Omega = 1 + e^{\mathcal{K}_\sigma} + e^{\mathcal{K}_\Omega} + \mathfrak{C}_{\sigma\Omega} e^{\mathcal{K}_\sigma + \mathcal{K}_\Omega}, \tag{4.3}$$

in the similar fashion the second-order dispersion coefficient $\mathfrak{R}_{12}$ can be expressed generally as

$$\mathfrak{R}_{\sigma\Omega} = \frac{\mathcal{P}_{\sigma\Omega}\lambda_\sigma + \mathcal{Q}_{\sigma\Omega}\lambda_\Omega + (\varrho_\sigma^4 + \varrho_\Omega^4)\alpha + (-4\varrho_\sigma^2 + 6\varrho_\sigma\varrho_\Omega - 4\varrho_\Omega)\varrho_\sigma\varrho_\Omega\alpha + (\varrho_\sigma - \varrho_\Omega)^3(\zeta_\sigma - \zeta_\Omega)\beta}{\mathcal{R}_{\sigma\Omega}(\lambda_\sigma + \lambda_\Omega) - (\varrho_\sigma^4 + \varrho_\Omega^4)\alpha + (-4\varrho_\sigma^2 - 6\varrho_\sigma\varrho_\Omega - 4\varrho_\Omega^2)\varrho_\sigma\varrho_\Omega\alpha - (\varrho_\sigma - \varrho_\Omega)^3(\zeta_\sigma + \zeta_\Omega)\beta}, \quad (4.4)$$

where $1 \le \sigma < \Omega \le 2$. Next to obtain the exact soliton solution of order two, we substitute Eq (4.1) with Eq (4.2) into Eqs (2.4) and (2.5) respectively, we obtained the following two second order solutions

$$\mathcal{U} = 2\left(-\frac{\left(\varrho_1 e^{\mathcal{K}_1} + \varrho_2 e^{\mathcal{K}_2} + (\varrho_1 + \varrho_2)\mathfrak{R}_{12}e^{\mathcal{K}_1+\mathcal{K}_2}\right)^2}{\mathcal{M}^2}\right.$$
$$\left.+\frac{\varrho_1^2 e^{\mathcal{K}_1} + \varrho_2^2 e^{\mathcal{K}_2} + (\varrho_1 + \varrho_2)^2\mathfrak{R}_{12}e^{\mathcal{K}_1+\mathcal{K}_2}}{\mathcal{M}}\right), \quad (4.5)$$

$$\mathcal{V} = 2\left(-\left(\frac{\left(\varrho_1 e^{\mathcal{K}_1} + \varrho_2 e^{\mathcal{K}_2} + (\varrho_1 + \varrho_2)\mathfrak{R}_{12}e^{\mathcal{K}_1+\mathcal{K}_2}\right)}{\mathcal{M}^2}\right.\right.$$
$$\left.\times\left(\zeta_1 e^{\mathcal{K}_1} + \zeta_2 e^{\mathcal{K}_2} + (\zeta_1 + \zeta_2)\mathfrak{R}_{12}e^{\mathcal{K}_1+\mathcal{K}_2}\right)\right) \quad (4.6)$$
$$\left.+\frac{\varrho_1\zeta_1 e^{\mathcal{K}_1} + \varrho_2\zeta_2 e^{\mathcal{K}_2} + (\varrho_1 + \varrho_2)(\zeta_1 + \zeta_2)\mathfrak{R}_{12}e^{\mathcal{K}_1+\mathcal{K}_2}}{\mathcal{M}}\right).$$

Where $\mathcal{M} = 1 + e^{\mathcal{H}_1} + e^{\mathcal{H}_2} + \mathfrak{R}_{12}e^{\mathcal{H}_1+\mathcal{H}_2}$. The first solution (4.5) is visualized in Figure 2, while the second solution (4.6) is graphically depicted in Figure 3 by using suitable parameters values. In these figures one can observe the X-type soliton solutions.
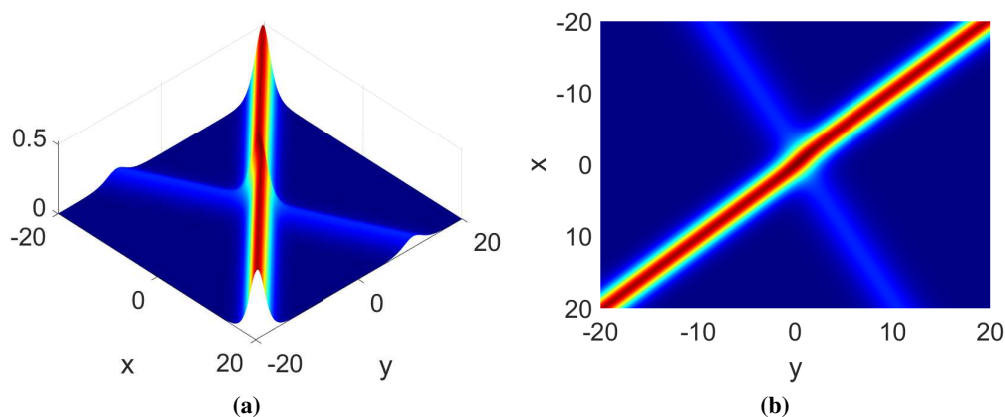

(a)

(b)

Figure 2. The 3D behavior of the second order soliton solution Eq (4.5) with parameters used as $z = 1$, $t = 1$, $\rho_1 = 0.4$, $\rho_2 = 1$, $\zeta_1 = -0.8$, $\zeta_2 = 1$, $\gamma_1 = 1$, $\gamma_2 = 1$, $\alpha = 1$, $\beta = 1$.
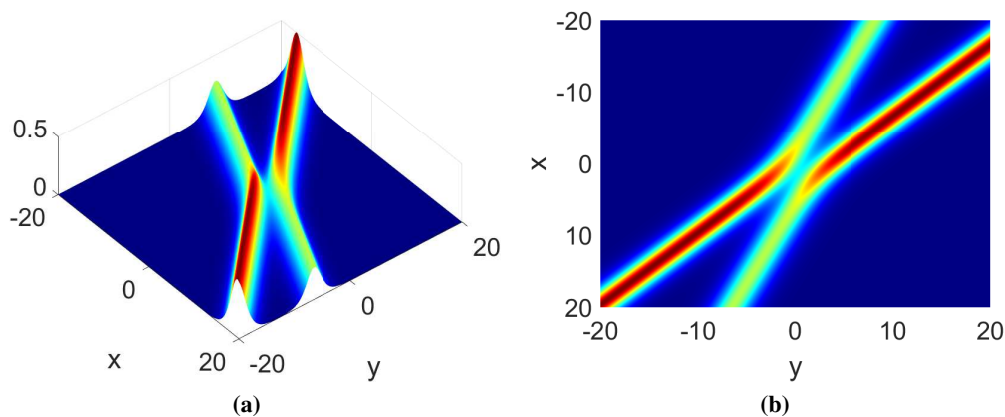
Figure 3. The 3D behavior of the second order soliton solution Eq (4.6) with parameters used as $z = 1$, $t = 1$, $\rho_1 = 0.5$, $\rho_2 = 1$, $\zeta_1 = 1.1$, $\zeta_2 = 1$, $\gamma_1 = 1$, $\gamma_2 = 1$, $\alpha = 1$, $\beta = 1$.

4.1. Bifurcation of second order soliton

In this part, we present the bifurcation in soliton of third order with the consideration of the dispersion coefficient $\Re_{12} = 0$ in Eq (5.1), therefore Υ takes the form

$$\Upsilon = 1 + e^{\mathcal{K}_1} + e^{\mathcal{K}_2}, \tag{4.7}$$

to get the bifurcation of soliton of order two, we first insert Eq (4.7) into Eq (2.4) and then into Eq (2.5). After obtaining the exact solutions we simulate them with consideration of proper values of parameters which are presented in Figures 4 and 5, where the y-type soliton is observed.
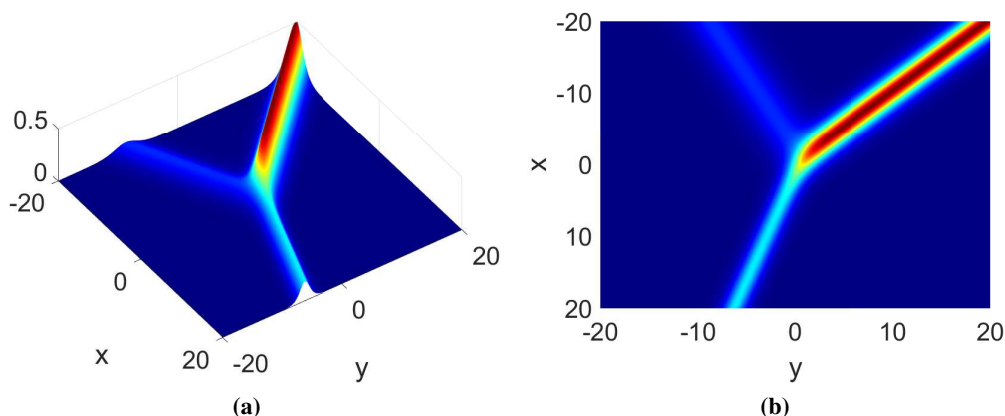

Figure 4. The 3D and 2D behavior of the y-type bifurcation in second order soliton solution with parameters used as $z = 1$, $t = 1$, $\rho_1 = 0.4$, $\rho_2 = 1$, $\zeta_1 = -0.8$, $\zeta_2 = 1$, $\gamma_1 = 1$, $\gamma_2 = 1$, $\alpha = 1$, $\beta = 1$.
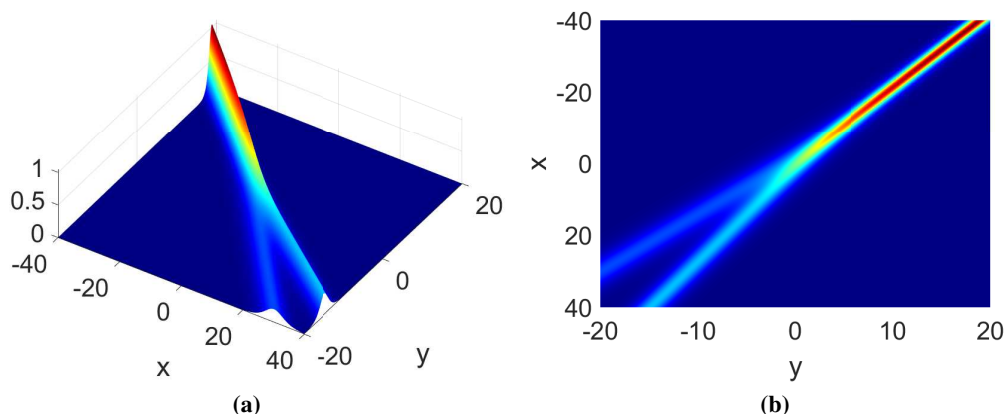
Figure 5. The 3D and 2D behavior of the y-type bifurcation in second order soliton solution with parameters used as $z = 1, t = 1, \rho_1 = 0.5, \rho_2 = 1, \zeta_1 = 1.1, \zeta_2 = 1, \gamma_1 = 0.8, \gamma_2 = 1, \alpha = 1, \beta = 1$.

5. Solitons of order three and bifurcation

In this part, we calculate and demonstrate the soliton solution of order three. To do so, we consider the function Υ in following form

$$\Upsilon = 1 + e^{\mathcal{K}_1} + e^{\mathcal{K}_2} + e^{\mathcal{K}_3} + \mathfrak{R}_{12}e^{\mathcal{K}_1+\mathcal{K}_2} + \mathfrak{R}_{13}e^{\mathcal{K}_1+\mathcal{K}_3} + \mathfrak{R}_{23}e^{\mathcal{K}_2+\mathcal{K}_3} + \mathfrak{R}_{123}e^{\mathcal{K}_1+\mathcal{K}_2+\mathcal{K}_3}, \quad (5.1)$$

where $\mathcal{K}_\varsigma, \varsigma = \{1, 2, 3\}$ follows from Eq (3.2). Further, one can verify that the $\mathfrak{R}_{123}$ satisfy the following relation

$$\mathfrak{R}_{123} = \mathfrak{R}_{12} \times \mathfrak{R}_{13} \times \mathfrak{R}_{23}. \quad (5.2)$$

Generally, the function Υ for the soliton of order three can be expressed as

$$\Omega = 1 + \sum_{\sigma=1}^{3} e^{\mathcal{K}_\sigma} + \mathfrak{C}_{\sigma\Omega}e^{\mathcal{K}_\sigma+\mathcal{K}_\Omega} + \mathfrak{C}_{\sigma\varphi}e^{\mathcal{K}_\sigma+\mathcal{K}_\varphi} + \mathfrak{C}_{\Omega\varphi}e^{\mathcal{K}_\Omega+\mathcal{K}_\varphi} + \mathfrak{C}_{\sigma\Omega\varphi}e^{\mathcal{K}_\sigma+\mathcal{K}_\Omega+\mathcal{K}_\varphi},$$

where $1 \leq \sigma < \Omega < \varphi$. The first soliton solution of order three can be acquired by inserting Eq (5.1) with Eq (5.2) into Eq (2.4). The graphical visualization of first solution with proper parameters is shown in the Figure 6. In similar way, the second soliton solution of order three can be acquired by putting Eq (5.1) with Eq (5.2) into Eq (2.5). The graphical visualization of second solution with proper parameters is shown in the Figure 7. In Figure 6, we have considered various values of ζ_3, where we observe its affects on the dynamics of wave. Similarly, in Figure 7, the ζ is varied which reveals that the increase in this parameter contracts the waves to small region.
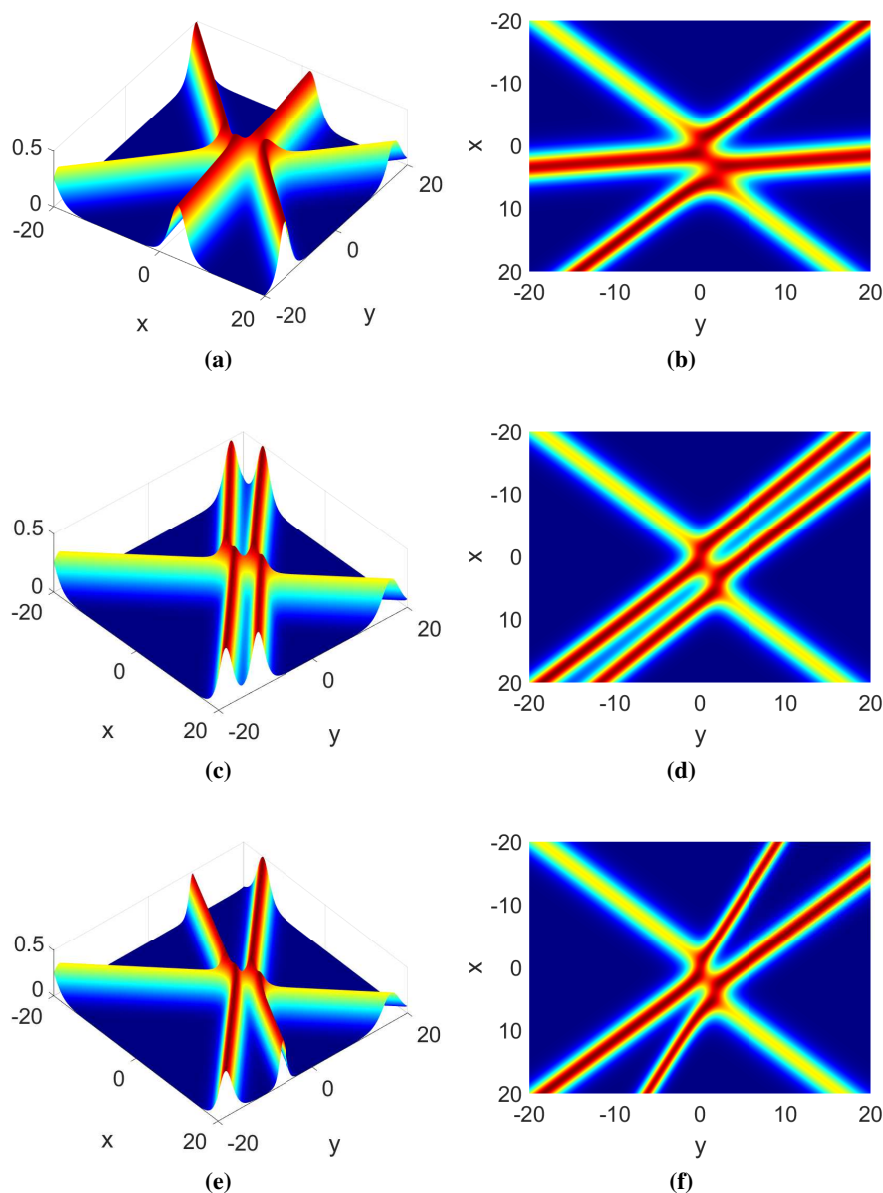
Figure 6. The 3D and 2D physical dynamics of the soliton solution of order three obtained by substituting Eq (5.1) with Eq (5.2) in Eq (2.4) with parameters considered as $z = t = \alpha = \beta = 1$, $\rho_1 = 0.8$, $\rho_2 = 1$, $\rho_3 = 0.98$ $\zeta_1 = -0.8$, $\zeta_2 = 1$, $\gamma_1 = \gamma_2 = \gamma_3 = 1$, and (a, b) $\zeta_3 = 0.1$, (c, d) $\zeta_3 = 1.1$, (e, f) $\zeta_3 = 2.1$.
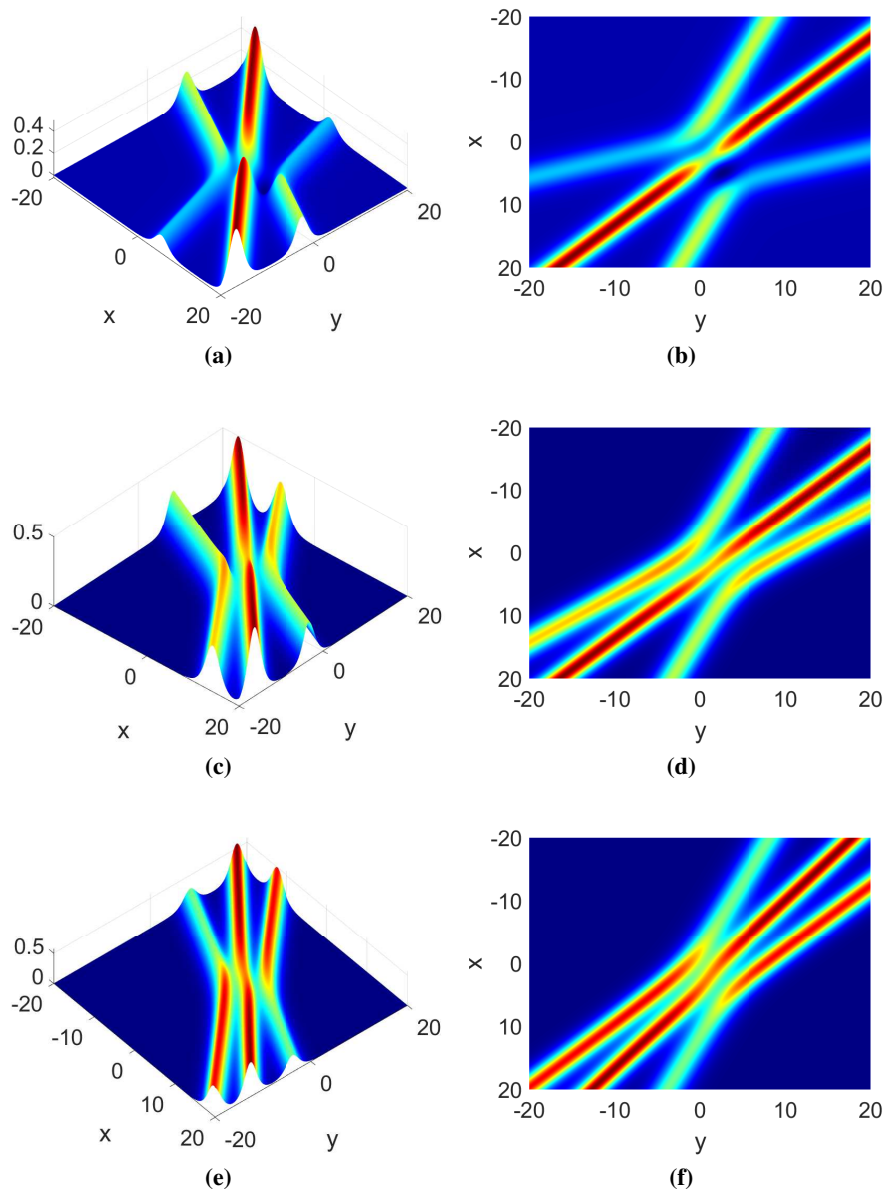
Figure 7. The 3D and 2D physical dynamics of the soliton of order three obtained by substituting Eq (5.1) with Eq (5.2) in Eq (2.5) with parameters considered as $z = t = \alpha = \beta = 1$, $\rho_2 = 1$, $\rho_1 = 0.5$, $\rho_3 = 0.95$ $\zeta_1 = 1.1$, $\zeta_2 = 1$, $\gamma_1 = \gamma_2 = \gamma_3 = 1$, and (a, b) $\zeta_3 = 0.3$, (c, d) $\zeta_3 = 0.7$, (e, f) $\zeta_3 = 1.2$.

5.1. Bifurcation of third order soliton

In this part, we would like to include the bifurcation of third order soliton by supposing the DC to be zero, and will see its affects on the dynamics of third order soliton of such supposition. So, first consider $\Re_{12} = 0$ in Eq (5.1), so Υ become

$$\Upsilon = 1 + e^{\mathcal{K}_1} + e^{\mathcal{K}_2} + e^{\mathcal{K}_3} + \Re_{13}e^{\mathcal{K}_1+\mathcal{K}_3} + \Re_{23}e^{\mathcal{K}_2+\mathcal{K}_3}, \tag{5.3}$$

where $\mathfrak{R}_{13}$ and $\mathfrak{R}_{23}$ can be collected from Eq (4.4). Next to get the bifurcation of third order soliton we insert Eq (5.3) into Eq (2.4), and after doing so graphically present the obtained result is depicted in Figure 8. Similarly to find the bifurcation of the second third order soliton, put Eq (5.3) into the Eq (2.5). The obtained result is graphically presented in Figure 9 with suitable parameters.
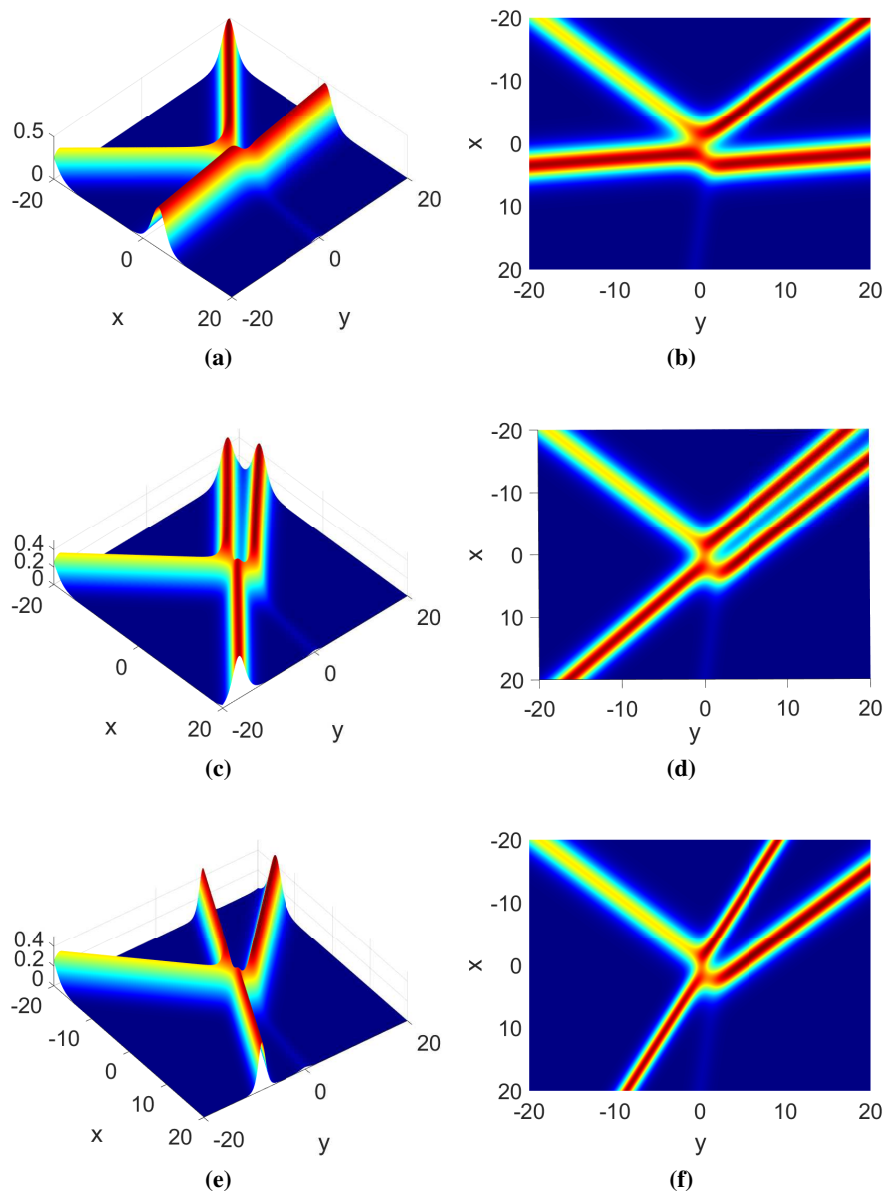

Figure 8. The 3D and 2D physical dynamics of the soliton solution of order three obtained with the insertion of Eq (5.3) with Eq (5.2) in Eq (2.4) with parameters considered as $z = t = \alpha = \beta = 1$, $\rho_1 = 0.8$, $\rho_2 = 1$, $\rho_3 = 0.98$ $\zeta_1 = -0.8$, $\zeta_2 = 1$, $\gamma_1 = \gamma_2 = \gamma_3 = 1$, and (a, b) $\zeta_3 = 0.1$, (c, d) $\zeta_3 = 1.1$, (e, f) $\zeta_3 = 2.1$.
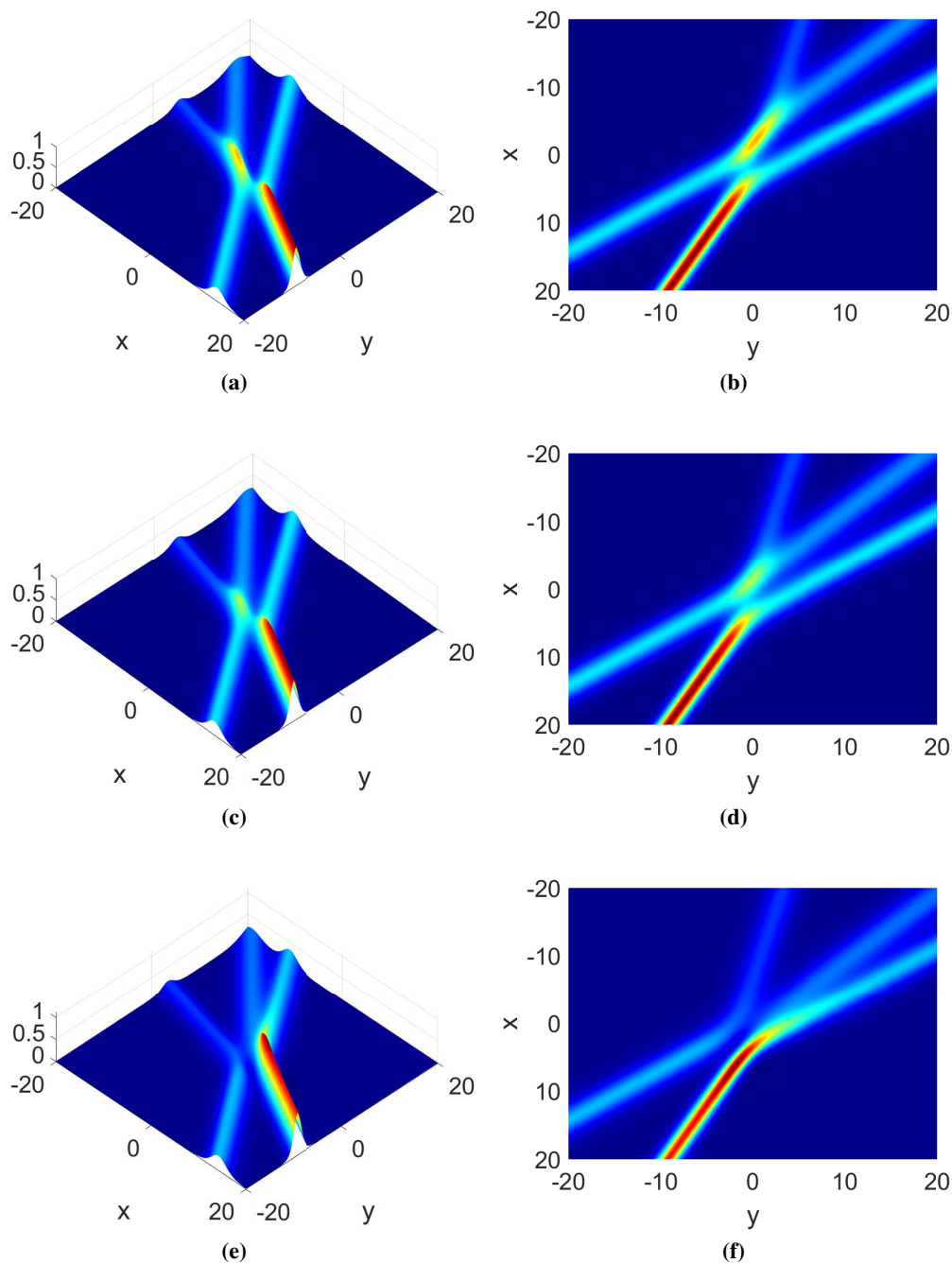
Figure 9. The 3D and 2D physical dynamics of the soliton solution of order three obtained with substituting Eq (5.3) along with Eq (5.2) in Eq (2.5) with parameters considered as $z = t = \alpha = \beta = 1$, $\rho_1 = 0.3$, $\rho_2 = 1$, $\rho_3 = 0.95$ $\zeta_1 = 1.2$, $\zeta_2 = 1.9$, $\zeta_3 = 0.7$, $\gamma_2 = 2$, $\gamma_3 = 1$, and (a, b) $\gamma_1 = -0.5$, (c, d) $\gamma_1 = 0.2$, (e, f) $\gamma_1 = 2$.

Further we set $\Re_{13} = 0$ in Eq (5.1), so that the auxiliary function Υ takes the form

$$\Upsilon = 1 + e^{\mathcal{K}_1} + e^{\mathcal{K}_2} + e^{\mathcal{K}_3} + \Re_{12} e^{\mathcal{K}_1 + \mathcal{K}_3} + \Re_{23} e^{\mathcal{K}_2 + \mathcal{K}_3}, \tag{5.4}$$

where the DCs $\Re_{12}$ and $\Re_{23}$ can be found from Eq (4.4). To observe the bifurcation with $\Re_{13} = 0$, we

insert Eq (5.4) into the Eq (2.4) and then into Eq (2.5) which are simulated with suitable parameters in Figures 10 and 11 respectively.
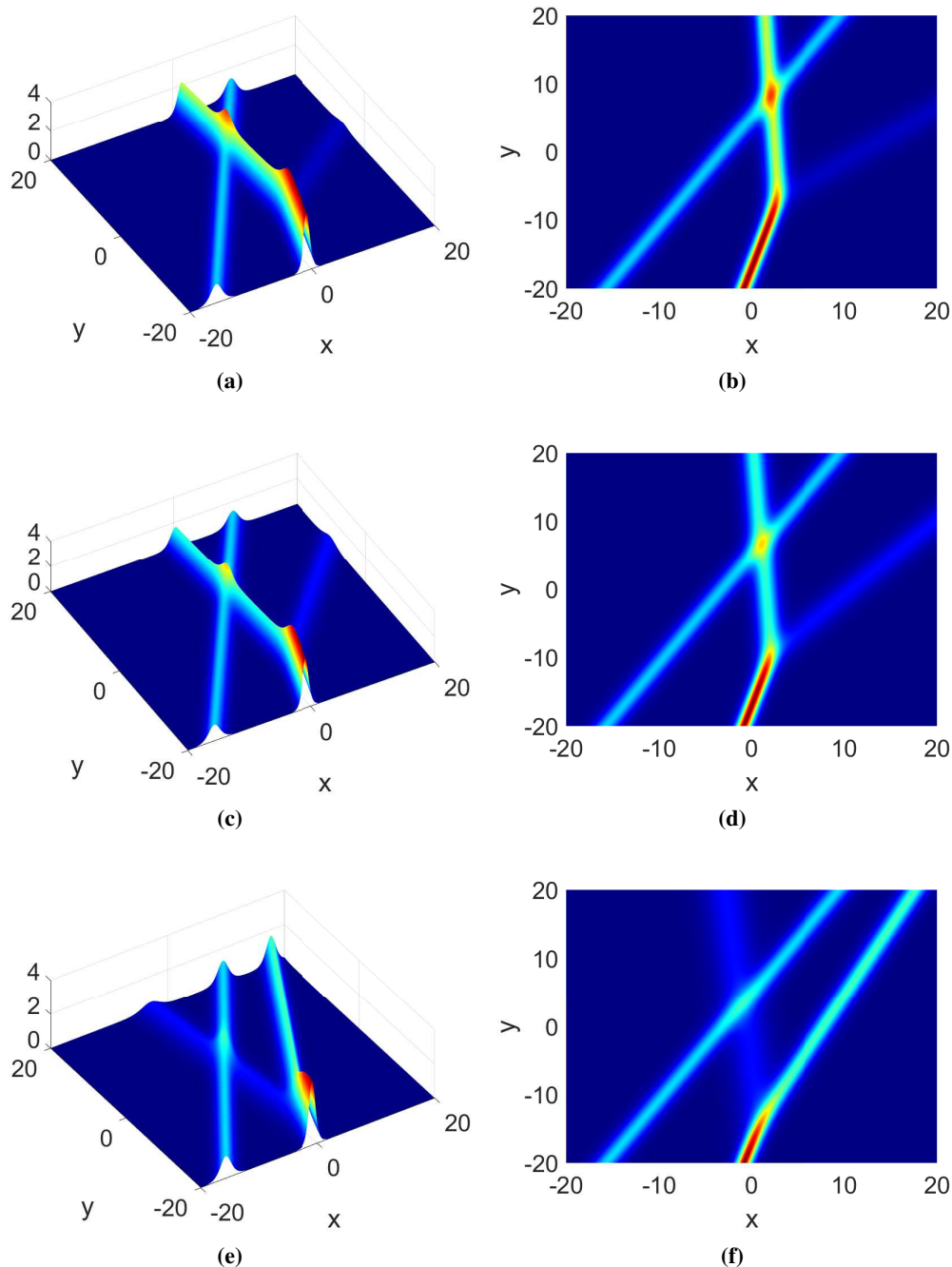

Figure 10. The 3D and 2D physical dynamics of the soliton of order three obtained by substitution of Eq (5.4) with Eq (5.2) in Eq (2.4) with parameters considered as $z = t = \alpha = \beta = 1$, $\rho_1 = 0.8$, $\rho_2 = 1$, $\zeta_1 = -0.8$, $\zeta_2 = 1$, $\zeta_3 = 0.1$, $\gamma_1 = \gamma_2 = \gamma_3 = 1$, and $(a, b) \rho_3 = 2.1$, $(c, d) \rho_3 = 1.8$, $(e, f) \rho_3 = 0.98$.
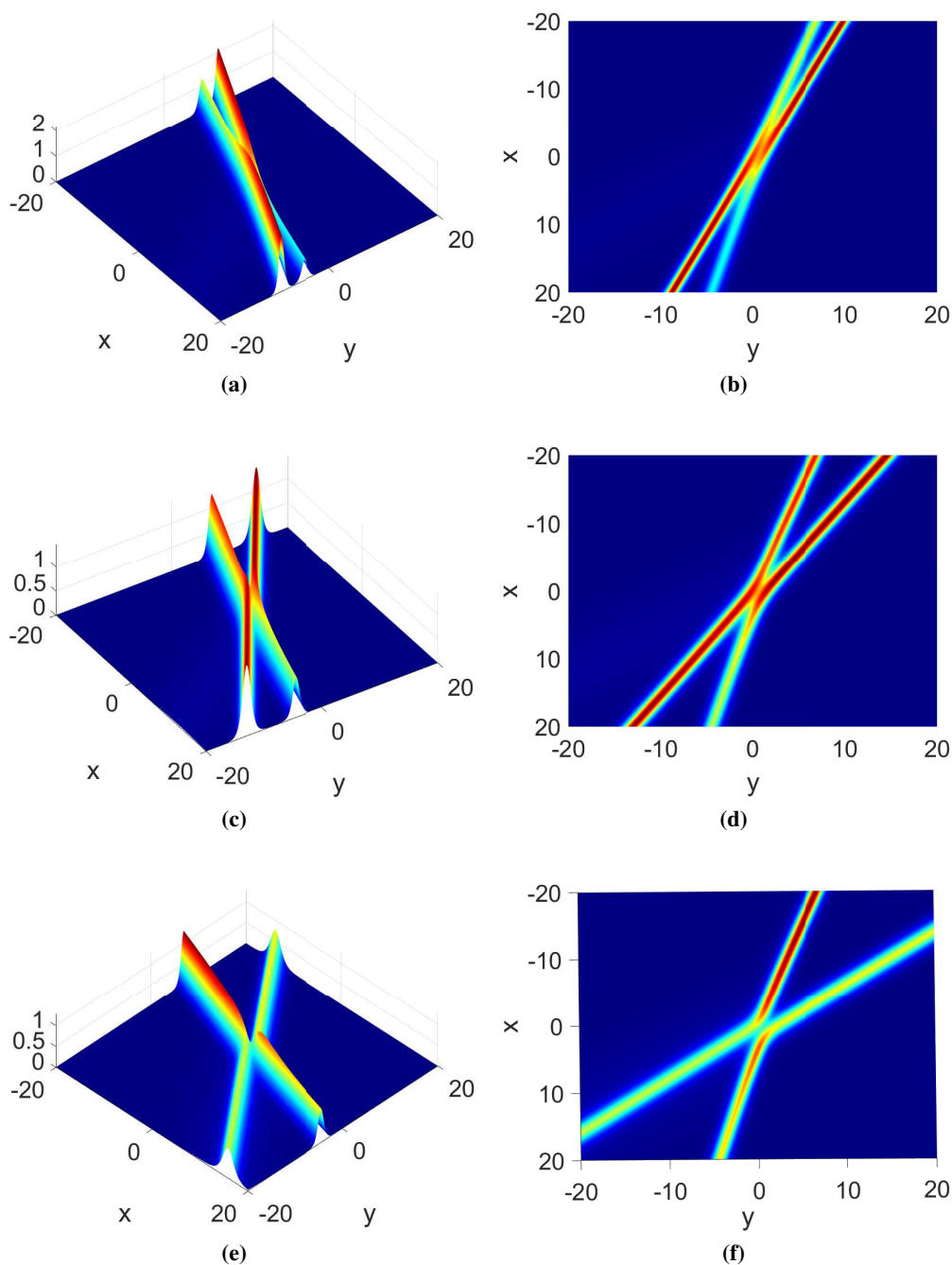
Figure 11. The 3D and 2D physical dynamics of the soliton solution of order three obtained with insertion of Eq (5.4) with Eq (5.2) in Eq (2.5) with parameters considered as $z = t = \alpha = \beta = 1$, $\rho_1 = 0.5$, $\rho_2 = 1$, $\rho_3 = 0.95$ $\zeta_1 = 1.1$, $\zeta_3 = 2.7$, $\gamma_1 = \gamma_2 = \gamma_3 = 1$, and (a, b) $\zeta_2 = 3.1$, (c, d) $\zeta_2 = 2.1$, (e, f) $\zeta_2 = 1.1$.

In Figure 8, it can be seen that at $\zeta_3 = 1.1$ the tuning fork shaped soliton is observed. Further, in Figure 9, complex type bifurcated soliton is observed. Figure 10 shows the combined x-y-type solitons dynamics and Figure 11 shows the x-type soliton solution.

6. Fourth order solitons with bifurcation

This part presents the supposition of Υ in a appropriate way to get fourth-order solitons solution of suggested Eq (1.1). To get so, we consider Υ as presented below:

$$\Upsilon = 1 + \sum_{\delta=1}^{4} e^{\mathcal{K}_\delta} + \sum_{1 \leq \delta < \Upsilon \leq 4} \Re_{\delta\Upsilon} e^{\mathcal{K}_\delta + \mathcal{K}_\Upsilon} + \sum_{1 \leq \delta < \Upsilon < \varphi \leq 4} \Re_{\delta\Upsilon\varphi} e^{\mathcal{K}_\delta + \mathcal{K}_\Upsilon + \mathcal{K}_\varphi} \qquad (6.1)$$
$$+ \Re_{1234} e^{\mathcal{K}_1 + \mathcal{K}_2 + \mathcal{K}_3 + \mathcal{K}_4},$$

where in Eq (6.1), $\Re_{\delta\Upsilon}$ follow Eq (4.4) and $\Re_{\delta\Upsilon\varphi}$ satisfy Eq (5.2). Moreover, it can be found that the fourth order DC satisfy:

$$\Re_{1234} = \Re_{12} \times \Re_{13} \times \Re_{14} \times \Re_{23} \times \Re_{24} \times \Re_{34}. \qquad (6.2)$$

One can obtain fourth-order solitons solution by substituting Eq (6.1) with Eq (6.2) in the Eqs (2.4) and (2.5). The graphical demonstrations of the fourth order solitons with suitable parameters are visualized in the Figures 12 and 13.
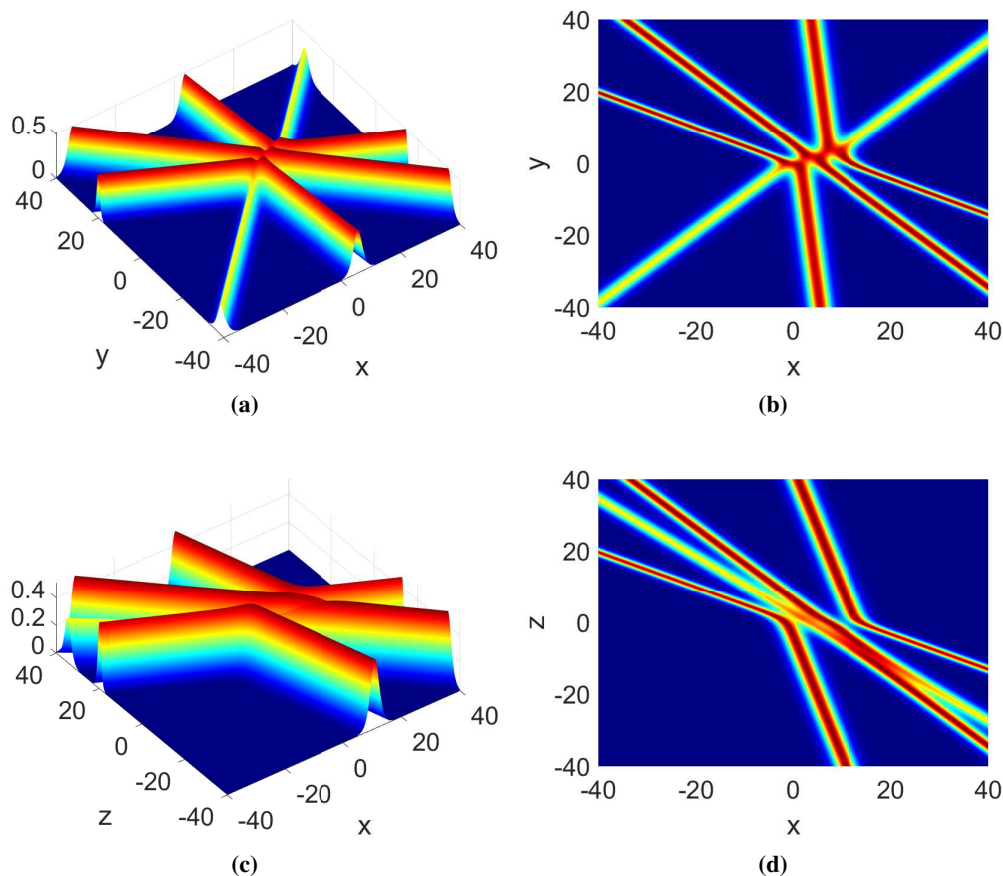

Figure 12. The 3D and 2D behavior of fourth-order solitons of Eq (2.4) with $z = t = \alpha = \beta = 1$, $\rho_1 = 0.5$, $\rho_2 = 1$, $\rho_3 = 0.95$, $\rho_4 = 0.95$ $\zeta_1 = 1.1$, $\zeta_3 = 2.7$, $\zeta_4 = 2.7$, $\gamma_1 = \gamma_2 = \gamma_3 = \gamma_4 = 1$, $[(a), (b)], \zeta_2 = 0.3$, $z = 0.5$ and $[(c), (d)], \zeta_2 = 0.8$, $y = 1$.
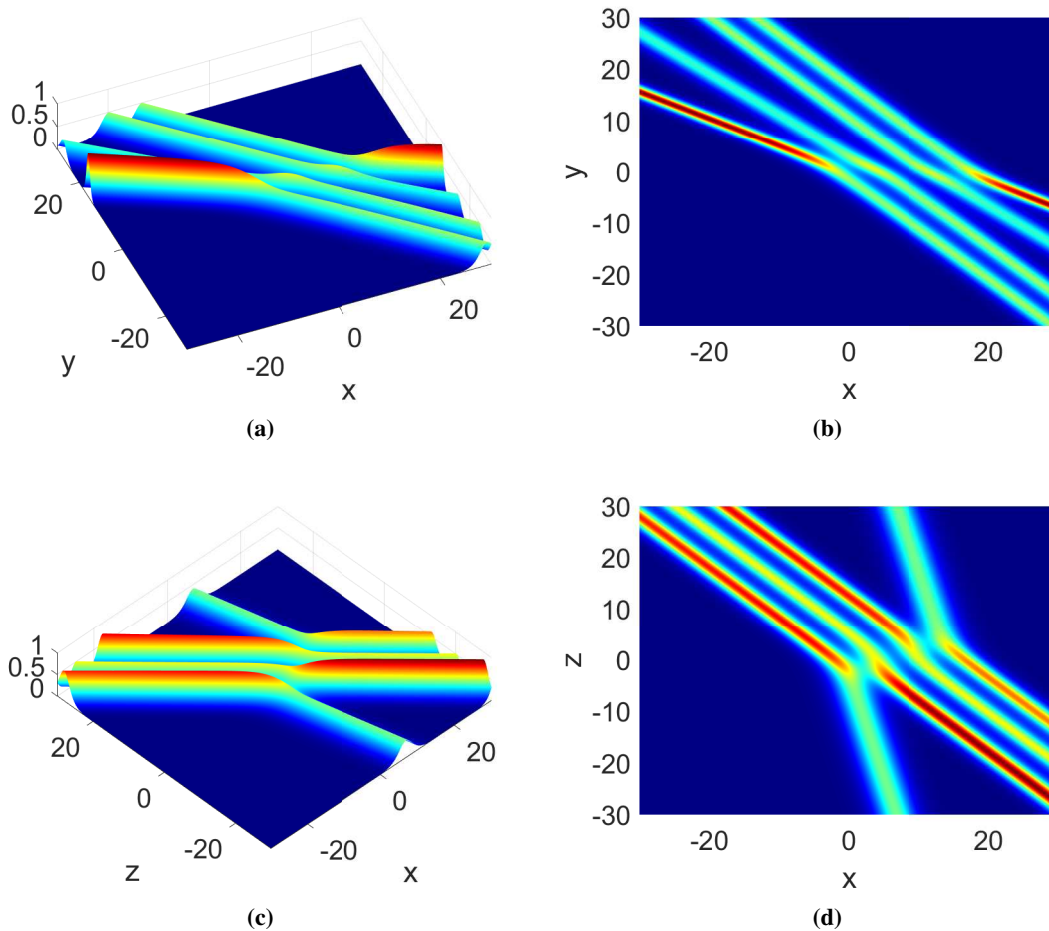
Figure 13. The 3D and 2D behavior of fourth-order solitons of Eq (2.5) with the parameters supposed as $t = \alpha = \beta = 1$, $\rho_1 = 0.5$, $\rho_2 = 1$, $\rho_3 = 0.95$, $\rho_4 = 0.95$ $\zeta_1 = 1.1$, $\zeta_3 = 2.7$, $\zeta_4 = 2.7$, $\gamma_1 = \gamma_2 = \gamma_3 = \gamma_4 = 1$, $[(a),(b)]$, $\zeta_2 = 0.3$, $z = 1$ and $[(c),(d)]$, $\zeta_2 = 0.8$, $y = 1$.

6.1. Bifurcation in fourth order solitons

Here, we suppose various dispersion coefficients as zeros due to which bifurcation is obtained of the suggested Eq (1.1). To do so, we suppose $\mathcal{R}_{12} = 0$ in the auxiliary function, so we obtain

$$\Upsilon = 1 + \sum_{\delta=1}^{4} e^{\mathcal{K}_\delta} + \mathcal{R}_{13} e^{\mathcal{K}_1 + \mathcal{K}_3} + \mathcal{R}_{14} e^{\mathcal{K}_1 + \mathcal{K}_2} + \mathcal{R}_{23} e^{\mathcal{K}_2 + \mathcal{K}_3} + \mathcal{R}_{24} e^{\mathcal{K}_2 + \mathcal{K}_4} + \mathcal{R}_{34} e^{\mathcal{K}_3 + \mathcal{K}_4} \tag{6.3}$$
$$+ \mathcal{R}_{134} e^{\mathcal{K}_1 + \mathcal{K}_3 + \mathcal{K}_4} + \mathcal{R}_{234} e^{\mathcal{K}_2 + \mathcal{K}_3 + \mathcal{K}_4},$$

where in Eq (6.3), $\mathfrak{R}_{134}$ and $\mathfrak{R}_{234}$ satisfy Eq (5.2). Solution of bifurcation of fourth-order solitons can be acquired by substituting Eq (6.3) in the Eqs (2.4) and (2.5). The physical demonstrations of the bifurcation of fourth order soliton with suitable parameters are visualized in the Figures 14 and 15. Further we suppose the DC $\mathcal{R}_{12} = \mathcal{R}_{23} = \mathcal{R}_{34}$ as zeros. So we get the following form of Υ

$$\Upsilon = 1 + \sum_{\delta=1}^{4} e^{\mathcal{K}_\delta} + \mathcal{R}_{13} e^{\mathcal{K}_1 + \mathcal{K}_3} + \mathcal{R}_{14} e^{\mathcal{K}_1 + \mathcal{K}_2} + \mathcal{R}_{24} e^{\mathcal{K}_2 + \mathcal{K}_4}. \tag{6.4}$$

Solution of bifurcation of fourth-order solitons can be acquired by substituting Eq (6.4) in the Eqs (2.4) and (2.5). The physical demonstrations of the bifurcation of fourth order soliton with suitable parameters are visualized in the Figures 16 and 17.
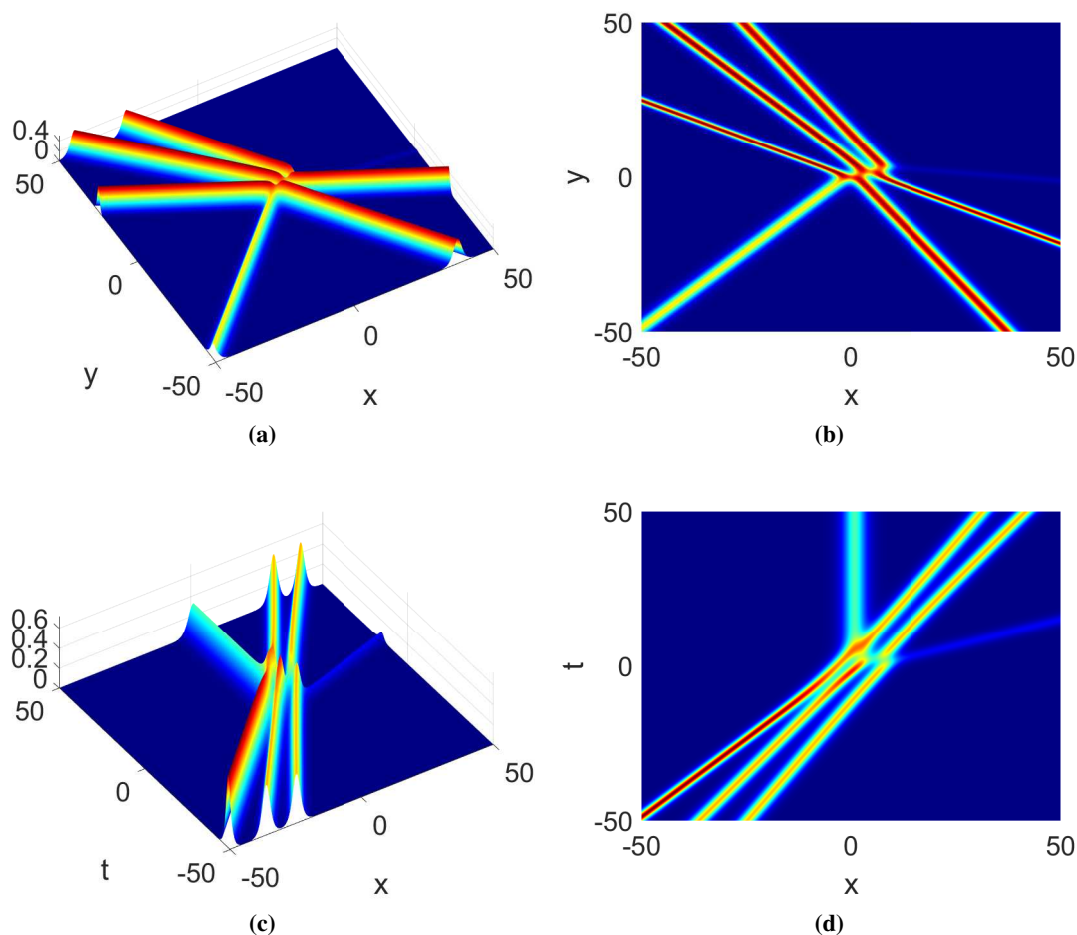

Figure 14. The 3D and 2D physical dynamics of bifurcation soliton solution of order four with parameters considered as $z = \alpha = \beta = 1$, $\rho_1 = 0.5$, $\rho_2 = 1$, $\rho_3 = 0.95$, $\rho_4 = 0.95$ $\zeta_1 = 1.1$, $\zeta_3 = 2.7$, $\zeta_4 = 2.7$, $\gamma_1 = \gamma_2 = \gamma_3 = \gamma_4 = 1$, $[(a), (b)]$, $\zeta_2 = 0.1$, $t = 1$ and $[(c), (d)]$, $\zeta_2 = 0.3$, $y = 1$.
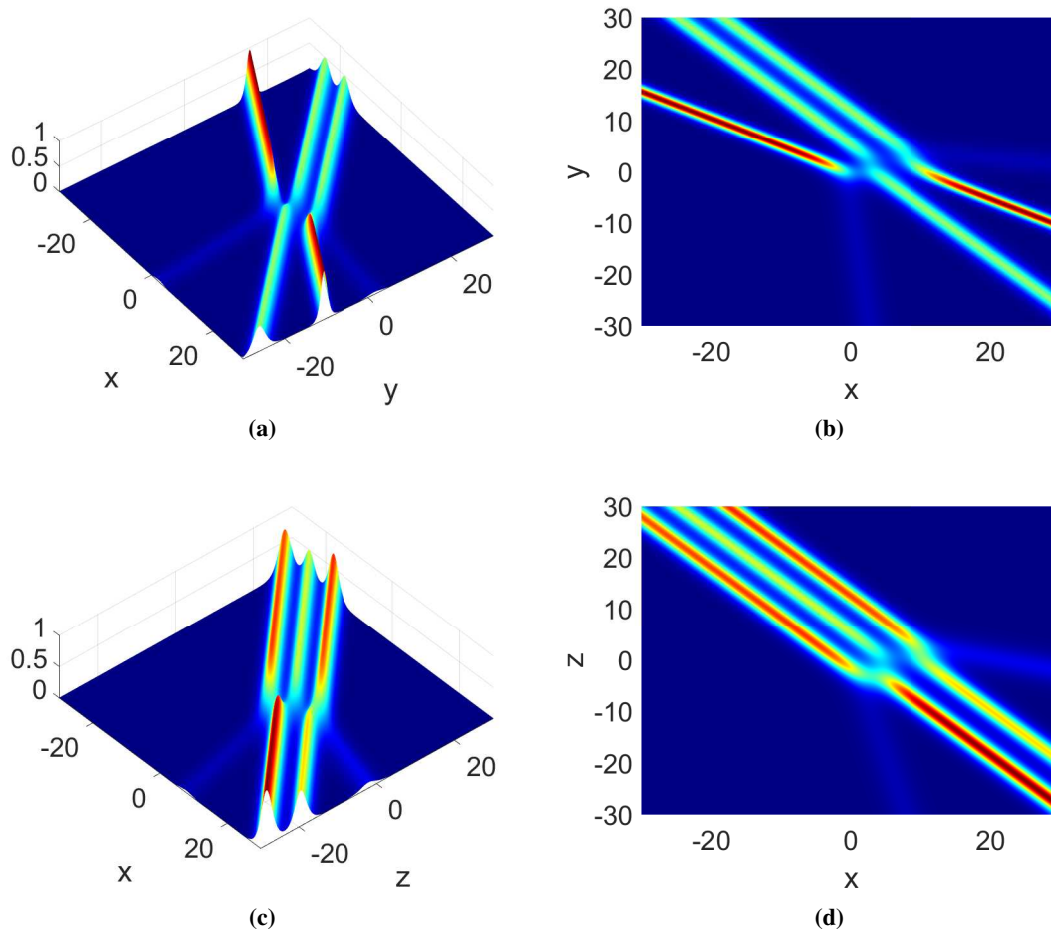
Figure 15. The 3D and 2D physical dynamics of the bifurcation solitons of order four with parameters considered as $t = \alpha = \beta = 1$, $\rho_1 = 0.5$, $\rho_2 = 1$, $\rho_3 = 0.95$, $\rho_4 = 0.95$ $\zeta_1 = 1.1$, $\zeta_3 = 2.7$, $\zeta_4 = 2.7$, $\gamma_1 = \gamma_2 = \gamma_3 = \gamma_4 = 1$, $[(a), (b)]$, $\zeta_2 = 0.3$, $z = 1$ and $[(c), (d)]$, $\zeta_2 = 0.8$, $y = 1$.
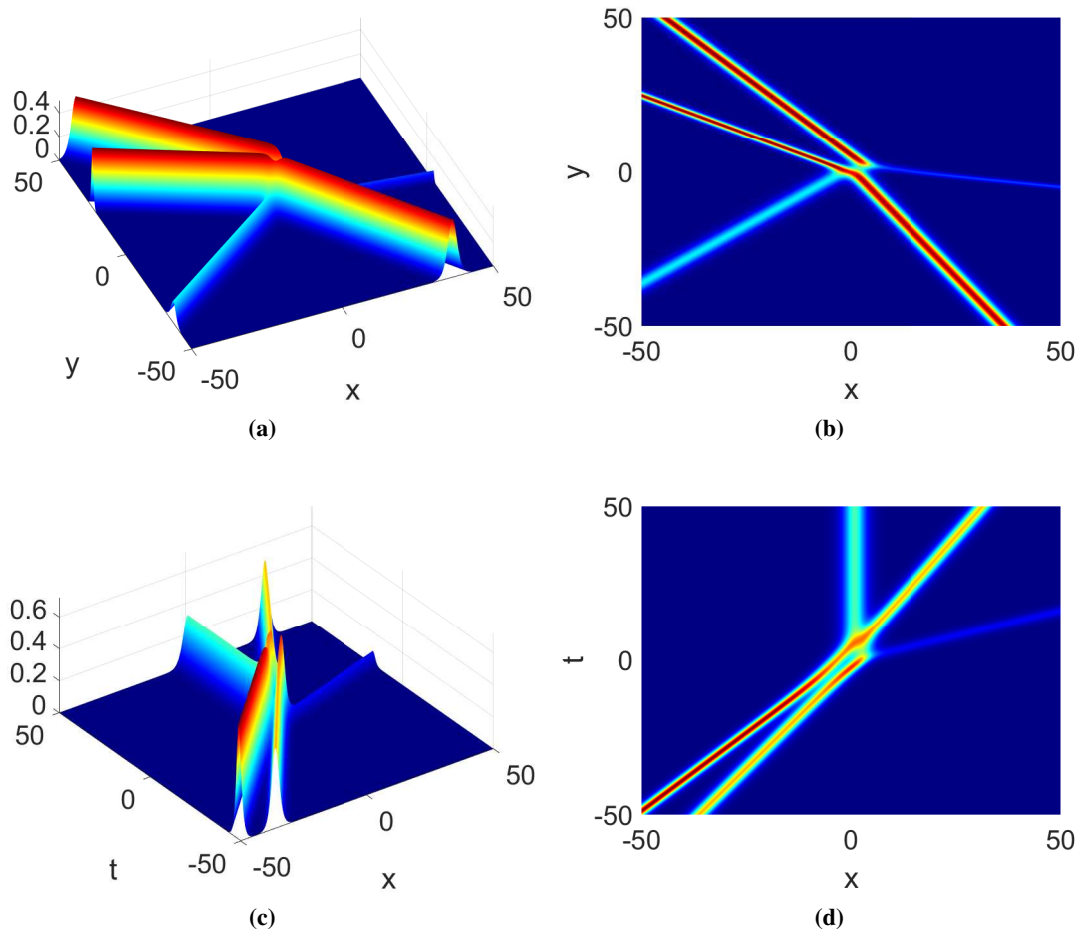
Figure 16. The 3D and 2D physical dynamics of bifurcation soliton solution of order four in Eq (2.4) with parameters considered as $z = \alpha = \beta = 1$, $\rho_1 = 0.5$, $\rho_2 = 1$, $\rho_3 = 0.99$, $\rho_4 = 1$ $\zeta_1 = -0.8$, $\zeta_2 = 1$, $\zeta_3 = 0.9$, $\zeta_4 = 2$, $\gamma_1 = 0.1$, $\gamma_2 = \gamma_3 = \gamma_4 = 1$, $[(a),(b)], \rho_1 = 0.6$, $t = 1$ and $[(c),(d)], \rho_1 = 0.8$, $y = 1$.
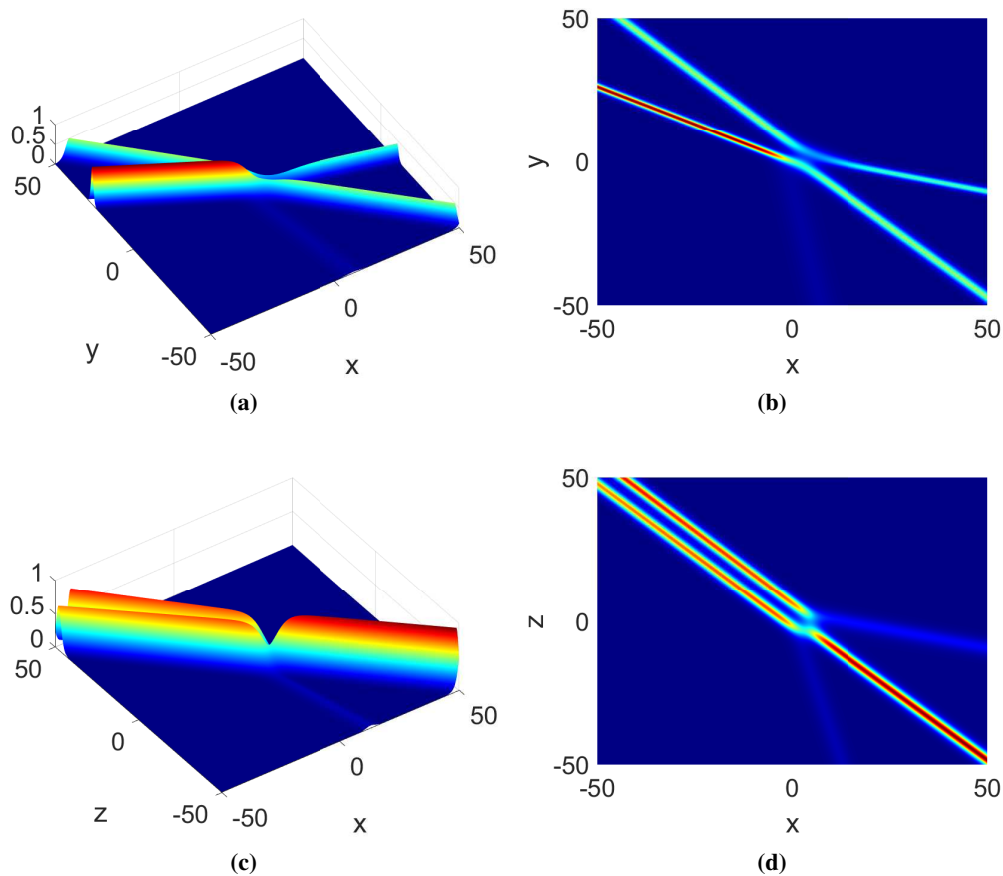
Figure 17. The 3D and 2D physical dynamics of the bifurcation solitons of order four with parameters considered as $t = \alpha = \beta = 1$, $\rho_2 = 1$, $\rho_3 = 0.98$, $\rho_4 = 1$ $\zeta_1 = 0.1$, $\zeta_2 = 1$, $\zeta_3 = 1$, $\zeta_4 = 1.9$, $\gamma_1 = \gamma_2 = \gamma_3 = \gamma_4 = 1$, $[(a), (b)]$, $\rho_1 = 0.55$, $z = 1$ and $[(c), (d)]$, $\rho_1 = 0.8, y = 1$.

7. Various soliton structures

In this section, we derive various soliton structures including lump wave, interaction and M as well as W shaped solitons with the consideration of suitable auxiliary functions.

7.1. Lump waves

This part presents the lump wave solutions of the suggested (3+1)-dimensional gBSS by choosing the transformation in the form [21, 22]

$$\Upsilon = (\varsigma_1 x + \varsigma_2 y + \varsigma_3 z + \varsigma_4 t + \varsigma_5)^2 + (\varsigma_6 x + \varsigma_7 y + \varsigma_8 z + \varsigma_9 t + \varsigma_{10})^2 + \varsigma_{11}. \tag{7.1}$$

On substituting Eq (7.1) in Eq 3.2, and equating the coefficients of variables x, y, z and t along with the combinations of them as well as various powers, we obtained a system comprised of algebraic

equations. The solution of the obtained system yields the following values

$$\alpha = -\frac{\beta\left(\varsigma_1\varsigma_2 - \varsigma_7^2 - \varsigma_7\varsigma_8\right)}{\varsigma_1^2 + \varsigma_7^2 + 2\varsigma_7\varsigma_8 + \varsigma_8^2}, \quad \varsigma_3 = -\varsigma_1 - \varsigma_2, \quad \varsigma_6 = -\varsigma_7 - \varsigma_8, \quad \varsigma_9 = -\frac{\varsigma_4\left(\varsigma_2^2 - \varsigma_7^2\right)}{2\varsigma_2\varsigma_7}. \tag{7.2}$$

Next inserting the parameter values Eq (7.2) into Eq (7.1), and then putting into Eqs (2.4) and (2.5) we obtained two exact solutions. The dynamics of the exact solutions Eqs (2.4) and (2.5) are presented in Figure 18 with suitable parameters.
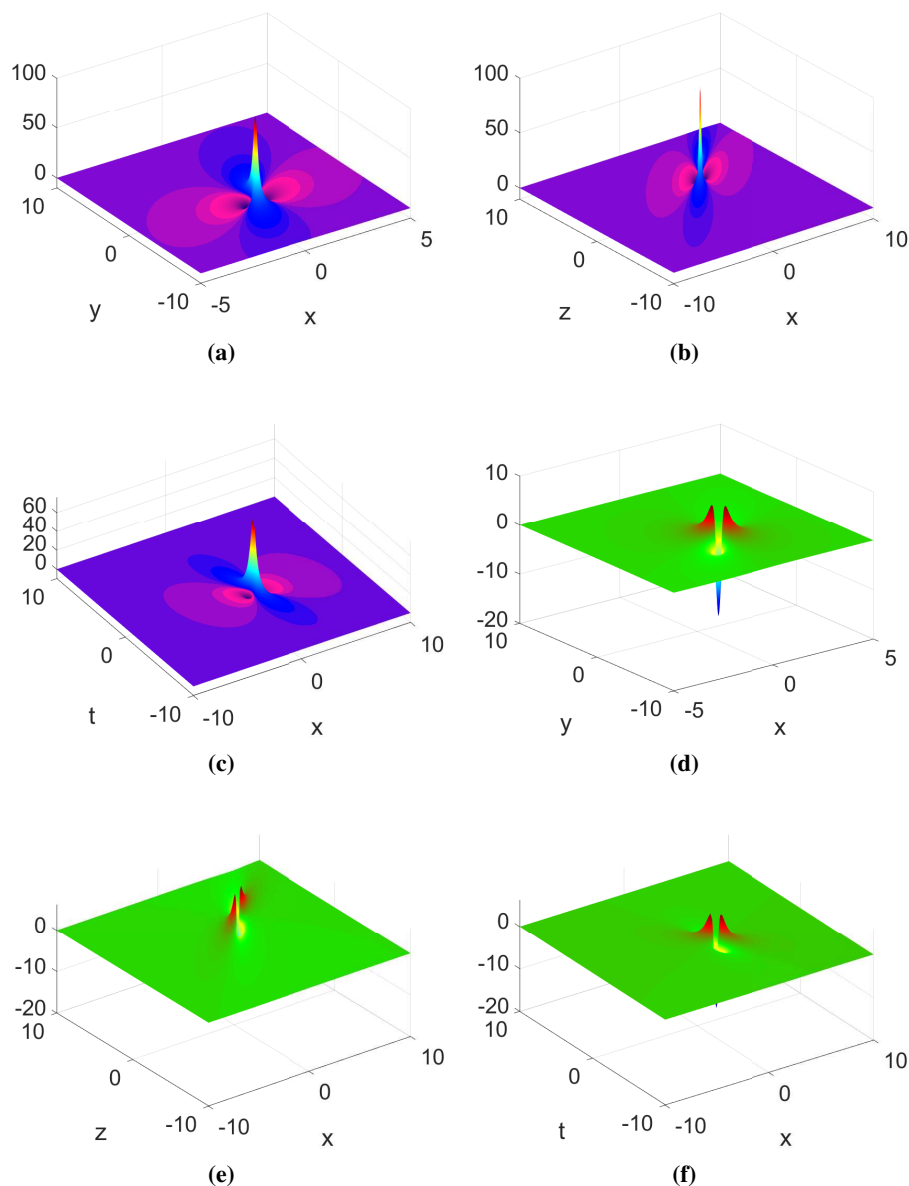

Figure 18. The visualization of lump wave solution in different planes with parameters used in the form $\varsigma_1 = 1, \varsigma_2 = 1, \varsigma_4 = 2, \varsigma_5 = 1, \varsigma_7 = 1, \varsigma_8 = 2, \varsigma_{10} = 1, \varsigma_{11} = .5$ and (a, d) $z = t = 1$, (b, e) $y = t = 1$, (c, f) $y = z = 1$.

7.2. Interaction of M-M shaped with dark soliton

In this, we aim to present the interaction of two M-shaped solitons with the dark soliton solution. For the achievement of our result we use the transformation in the following form

$$
\begin{aligned}
\Upsilon \;=\; & e^{\varsigma_1 x + \varsigma_2 y + \varsigma_3 t + + \varsigma_4 t + \varsigma_5} + cos(\varsigma_6 x + \varsigma_7 y + \varsigma_8 z + \varsigma_9 t + \varsigma_{10} + \varsigma_{11}) \\
& + cosh(\varsigma_{12} x + \varsigma_{13} y + \varsigma_{14} t + \varsigma_{15}).
\end{aligned} \tag{7.3}
$$

Next, inserting Eq (7.3) into Eq (3.2), and equating the like powers and of the exponential, trigonometric and hyperbolic functions along with the combinations of them, we obtained system comprised of algebraic equations. On solving the algebraic system, we obtain following:

$$
\varsigma_1 = 0, \; \varsigma_3 = -\frac{\varsigma_2\left(\varsigma_{11}^3 \beta + \varsigma_{14}\right)}{\varsigma_{14}}, \; \varsigma_4 = 0, \; \varsigma_6 = 0, \; \varsigma_8 = -\frac{\varsigma_7\left(\varsigma_{11}^3 \beta + \varsigma_{14}\right)}{\varsigma_{14}}, \; \varsigma_9 = 0, \; \varsigma_{12} = -\frac{\alpha\varsigma_{11}}{\beta},
$$

$$
\varsigma_{13} = \frac{\varsigma_{11}(\alpha - \beta)}{\beta}. \tag{7.4}
$$

Here the parameters ς_{14} and β should be greater than 0. Further, inserting the parameter values Eq (7.4) into Eq (7.3), and then putting into Eqs (2.4) and (2.5) we obtained two exact solutions of the interaction. The interaction of M-M and dark soliton solutions are presented in Figure 19.
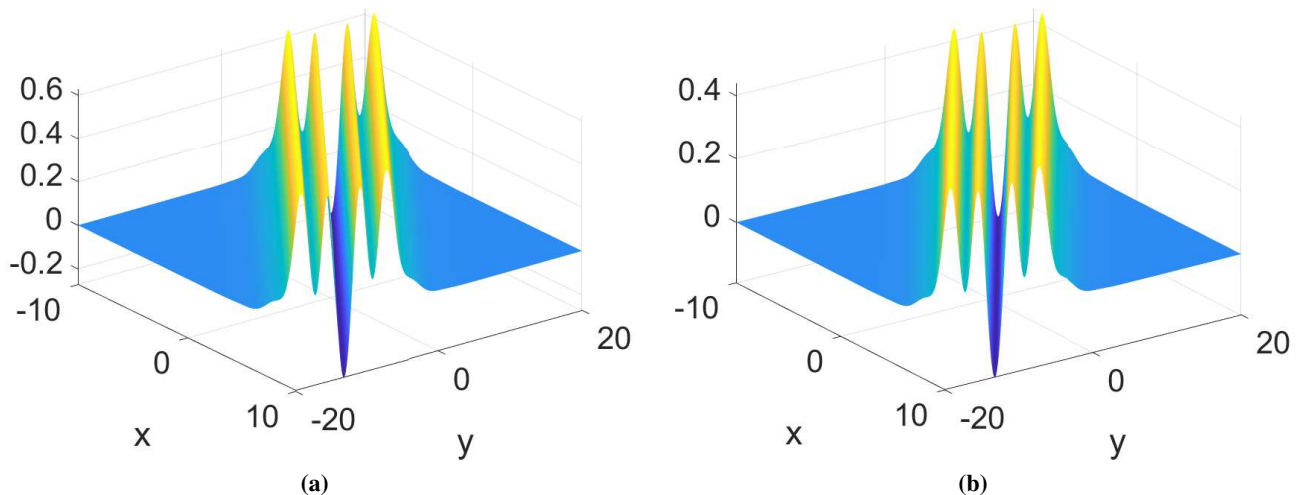

Figure 19. The visualization of M-M and dark soliton interaction with parameters used in the form $z = 1, t = 1, \varsigma_2 = .1, \varsigma_5 = 2, \varsigma_7 = .1, \varsigma_{10} = 1, \varsigma_{11} = 1, \varsigma_{15} = 1,$.

7.3. M and W shaped solitons

In this part of manuscript, we study the M-shaped and W-shaped soliton solutions. To reach the goal, we use the transformation in the following form

$$
\Upsilon = cos(\varsigma_1 x + \varsigma_3 y + \varsigma_4 z + \varsigma_5 t + \varsigma_6) + cosh(\varsigma_z x + \varsigma_8 y + \varsigma_9 z + \varsigma_{10} t + \varsigma_{11}). \tag{7.5}
$$

On putting Eq (7.5) into Eq (3.2), and comparing the coefficients of same powers of the hyperbolic and trigonometric functions along with the combinations of them, we obtained a system comprised of

algebraic equations. On solving the algebraic system gives:

$$\varsigma_2 = -\frac{\alpha\varsigma_1}{\beta}, \ \varsigma_3 = \frac{\varsigma_1(\alpha-\beta)}{\beta}, \ \varsigma_7 = -\frac{\alpha\varsigma_6}{\beta}, \ \varsigma_8 = \frac{\varsigma_6(\alpha-\beta)}{\beta}. \tag{7.6}$$

Here $\beta \neq 0$. Further, inserting the parameter values presented in Eq (7.6) into Eq (7.5), and then putting into Eqs (2.4) and (2.5) we obtained two exact solutions of M and W shaped respectively, which are simulated in Figure 20.
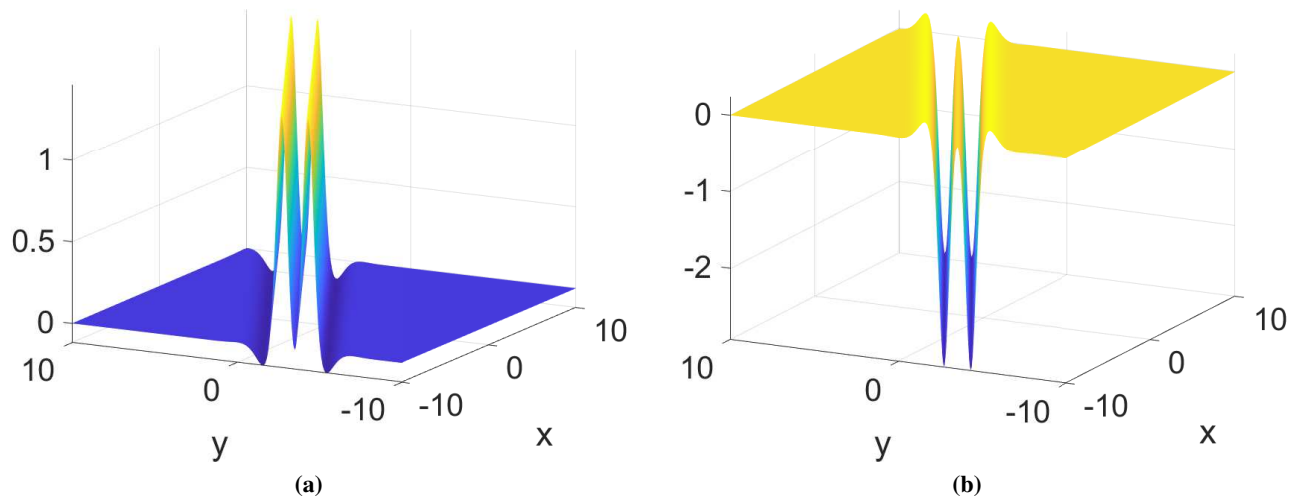

Figure 20. The visualization of M and W shaped solitons with parameters used in the form $z = 1, t = 1, \varsigma_1 = 1, \varsigma_4 = 1, \varsigma_5 = 1, \varsigma_6 = 1, \varsigma_9 = 1, \varsigma_{10} = 1, \varsigma_{11} = 1, \alpha = 1, \beta = .5.$

8. Conclusions

In the context of nonlinear evolution processes, it is not uncommon for certain characteristics to display unusual and remarkable properties. Our study has revealed that the displacement of solitons exhibits asymmetric resonant phenomena before and after bifurcation in a system defined by gBSS. This suggests that during interactions, the energy reflected by the amplitudes may shift. To explore this, we employed the Hirota bilinear approach to study gBSS and obtained novel solutions by considering different types of auxiliary functions. Our analysis includes the study of multi-solitons, multiple bifurcations solitons, lump wave, M-shaped solitons, and the interaction of M-M shaped with dark soliton. Additionally, we observed several novel hybrid solitons, such as tuning fork-shaped, X-Y shaped, and double Y shaped solitons.

Use of AI tools declaration

The authors declare they have not used Artificial Intelligence (AI) tools in the creation of this article.

Conflict of interest

All authors declare that they have no conflict of interest.

References

1. W. X. Ma, Riemann-Hilbert problems and soliton solutions of type $(-\lambda, \lambda)$ reduced nonlocal integrable mKdV hierarchies, *Mathematics*, **10** (2022), 870. https://doi.org/10.1088/1572-9494/ac75e0

2. J. Wu, A direct reduction approach for a shifted nonlocal nonlinear Schrödinger equation to obtain its N-soliton solution, *Nonlinear Dyn.*, **108** (2022), 4021–4028. https://doi.org/10.1007/s11071-022-07354-1

3. K. Hosseini, M. Samavat, M. Mirzazadeh, S. Salahshour, D. Baleanu, A new (4+1)-dimensional Burgers equation: Its backlund transformation and real and complex N-kink solitons, *Int. J. Appl. Comput. Math.*, **8** (2022), 172. https://doi.org/10.1007/s40819-022-01359-5

4. Y. X. Ma, B. Tian, Q. X. Qu, C. C. Wei, X. Zhao, Backlund transformations, kink soliton, breather- and travelling-wave solutions for a (3+1)-dimensional B-type Kadomtsev-Petviashvili equation in fluid dynamics, *Chin. J. Phys.*, **73** (2021), 600–612. https://doi.org/10.1016/j.cjph.2021.07.001

5. B. Q. Li, Y. L. Ma, Multiple-lump waves for a (3+1)-dimensional Boiti-Leon-Manna-Pempinelli equation arising from incompressible fluid, *Comput. Math. Appl.*, **76** (2018), 204–214. https://doi.org/10.1016/j.camwa.2018.04.015

6. M. S. Osman, A. M. Wazwaz, A general bilinear form to generate different wave structures of solitons for a (3+1)-dimensional Boiti-Leon-Manna-Pempinelli equation, *Math. Methods Appl. Sci.*, **42** (2019), 6277–6283. https://doi.org/10.1002/mma.5721

7. X. Yang, Z. Zhang, A. M. Wazwaz, Z. Wang, A direct method for generating rogue wave solutions to the (3+1)-dimensional Korteweg-de Vries Benjamin-Bona-Mahony equation, *Phys. Lett. A*, **449** (2022), 128355. https://doi.org/10.1016/j.physleta.2022.128355

8. Y. L. Ma, B. Q. Li, Interactions between rogue wave and soliton for a (2+1)-dimensional generalized breaking soliton system: Hidden rogue wave and hidden soliton, *Comput. Math. Appl.*, **78** (2019), 827–839. https://doi.org/10.1016/j.camwa.2019.03.002

9. H. Wang, Lump and interaction solutions to the (2+1)-dimensional Burgers equation, *Appl. Math. Lett.*, **85** (2018), 27–34. https://doi.org/10.1016/j.aml.2018.05.010

10. L. Cheng, Y. Zhang, W. X. Ma, Wronskian *N*-soliton solutions to a generalized KdV equation in (2+1)-dimensions, *Nonlinear Dyn.*, **111** (2023), 1701–1714. https://doi.org/10.1007/s11071-022-07920-7

11. D. Bilman, R. Buckingham, D. S. Wang, Far-field asymptotics for multiple-pole solitons in the large-order limit, *J. Differ. Equ.*, **297** (2021), 320–369. https://doi.org/10.1016/j.jde.2021.06.016

12. D. S. Wang, X. Zhu, Long-time asymptotics of the good Boussinesq equation with q xx-term and its modified version, *J. Math. Phys.*, **63** (2022), 123501. https://doi.org/10.1063/5.0118374

13. W. X. Ma, Dynamics of mixed lump-solitary waves of an extended (2+1)-dimensional shallow water wave model, *Phys. Lett. A*, **382** (2018), 3262–3268. https://doi.org/10.1016/j.physleta.2018.09.019

14. L. G. Huang, L. H. Pang, P. Wong, Y. Q. Li, S. Y. Bai, M. Lei, W. J. Liu, Analytic soliton solutions of cubic-quintic Ginzburg-Landau equation with variable nonlinearity and spectral filtering in fiber lasers, *Ann. Phys. Berlin*, **528** (2016), 493–503. https://doi.org/10.1002/andp.201500322

15. Y. L. Ma, A. M. Wazwaz, B. Q. Li, Novel bifurcation solitons for an extended Kadomtsev-Petviashvili equation in fluids, *Phys. Lett. A*, **413** (2021), 127585. https://doi.org/10.1016/j.physleta.2021.127585

16. B. Q. Li, Loop-like kink breather and its transition phenomena for the Vakhnenko equation arising from high-frequency wave propagation in electromagnetic physics, *Appl. Math. Lett.*, **112** (2021), 106822. https://doi.org/10.1016/j.aml.2020.106822

17. S. Ahmed, A. R. Seadawy, S. T. R. Rizvi, Study of breathers, rogue waves and lump solutions for the nonlinear chains of atoms, *Opt. Quantum Electron.*, **54** (2022), 320. https://doi.org/10.1007/s11082-022-03732-6

18. L. Kaur, A. M. Wazwaz, Bright-dark lump wave solutions for a new form of the (3+1)-dimensional BKP-Boussinesq equation, *Rom. Rep. Phys.*, **71** (2019), 1–11. https://doi.org/10.1108/HFF-07-2018-0405

19. S. T. R. Rizvi, M. Younis, D. Baleanu, H. Iqbal, Lump and rogue wave solutions for the Broer-Kaup-Kupershmidt system, *Chin. J. Phys.*, **68** (2020), 19–27. https://doi.org/10.1016/j.cjph.2020.09.004

20. A. R. Seaway, S. T. R. Rizvi, A. Ahmad, S. Ahmed, Multiwave, rogue wave, periodic wave, periodic cross-lump wave, periodic cross-kink wave, lump soliton, breather lump, homoclinic breather, periodic cross-kink, M-shaped rational solutions and their interactions for the Degasperis-Procesi equation, *Int. J. Mod. Phys. B*, 2023, 2350172. https://doi.org/10.1142/S0217979223501722

21. Y. Liu, X. Y. Wen, D. S. Wang, The N-soliton solution and localized wave interaction solutions of the (2+1)-dimensional generalized Hirota-Satsuma-Ito equation, *Comput. Math. Appl.*, **77** (2019), 947–966. https://doi.org/10.1016/j.camwa.2018.10.035

22. Y. Liu, X. Y. Wen, D. S. Wang, Novel interaction phenomena of localized waves in the generalized (3+1)-dimensional KP equation, *Comput. Math. Appl.*, **78** (2019), 1–19. https://doi.org/10.1016/j.camwa.2019.03.005